

# ENVIRONMENTAL CONTROLS OF PHOTOSYNTHETIC PARAMETERS IN FOUR DOMINANT BOREAL TREE SPECIES: CONTRASTING RESPONSES OF DECIDUOUS ANGIOSPERMS AND EVERGREEN GYMNOSPERMS

**Vladislava B. Pridacha<sup>1,\*</sup>, Alexander V. Olchev<sup>2</sup>**

<sup>1</sup>Forest Research Institute, Karelian Research Centre, Russian Academy of Sciences, Pushkinskaya St., 11, Petrozavodsk, 185910, Russia

<sup>2</sup>Faculty of Geography, Lomonosov Moscow State University, GSP-1, Leninskie Gory, Moscow, 119991, Russia

\*Corresponding author: [pridacha@krc.karelia.ru](mailto:pridacha@krc.karelia.ru)

Received: September 28<sup>th</sup> 2025 / Accepted: November 12<sup>nd</sup> 2025 / Published: December 31<sup>st</sup> 2025

<https://doi.org/10.24057/2071-9388-2025-4190>

**ABSTRACT.** Boreal forests play a crucial role in maintaining the global ecological balance, acting as significant carbon sinks and mitigating the effects of climate change. This study examined how temperature affects photosynthesis in four boreal tree species – *Pinus sylvestris*, *Betula pendula*, *Populus tremula*, and *Alnus incana* – growing in a clear-cut of mid-taiga bilberry-type pine forest in southern Karelia, Russia. The Farquhar biochemical model was used to analyze key photosynthesis parameters, such as the maximum carboxylation rate by Rubisco ( $V_{C_{max}}$ ), the maximum photosynthetic electron transport rate ( $J_{max}$ ), and the triose phosphate utilization (TPU) rate, under different leaf temperatures ranging from 20 to 35°C and light conditions. The results revealed significant interspecific differences in photosynthetic responses. At a leaf surface temperature of 25°C, the lowest  $V_{C_{max25}}$ ,  $J_{max25}$ , and TPU<sub>25</sub> values were obtained for the 1-year-old needles of *P. sylvestris* (38.8, 70.7, and 5.5  $\mu\text{mol m}^{-2} \text{s}^{-1}$ ), whereas the values were 1.5- to 2.4-fold higher for the leaves of *B. pendula* (93.5, 172.1, and 12.7  $\mu\text{mol m}^{-2} \text{s}^{-1}$ ), *A. incana* (86.1, 155.1, and 11.4  $\mu\text{mol m}^{-2} \text{s}^{-1}$ ), and *P. tremula* (58.6, 122, and 9.3  $\mu\text{mol m}^{-2} \text{s}^{-1}$ ). Meanwhile, *P. sylvestris* and *B. pendula* had a broader optimal temperature range for  $V_{C_{max}}$  and  $J_{max}$  (20–35°C), whereas *A. incana* and *P. tremula* had a narrower range (20–30°C), experiencing a decline at 35°C. In addition to having different levels of resistance to extreme temperatures, deciduous species also differed in their responsiveness to  $\text{CO}_2$  enrichment. This could lead to shifts in the composition of boreal forest species under changing climate conditions. *P. sylvestris* demonstrated greater stability at low light levels and a strong response to elevated  $\text{CO}_2$ , indicating its high adaptability to future climate change. These results highlight the importance of considering species characteristics when predicting the carbon balance of boreal forests. They can be used to model the resilience of forest ecosystems under climate change and to plan further investigations, including studies of mature trees and the effects of additional stress factors, such as drought.

**KEYWORDS:** boreal forests; photosynthetic  $\text{CO}_2$  response curve; photosynthetic light response curve; temperature dependence; climate change

**CITATION:** Pridacha V. B., Olchev A. V. (2025). Environmental Controls Of Photosynthetic Parameters In Four Dominant Boreal Tree Species: Contrasting Responses Of Deciduous Angiosperms And Evergreen Gymnosperms. *Geography, Environment, Sustainability*, 4 (18), 92-102

<https://doi.org/10.24057/2071-9388-2025-4190>

**ACKNOWLEDGEMENTS:** The study was funded from the federal budget within state assignment to the Karelian Research Centre, Russian Academy of Sciences (Forest Research Institute KarRC RAS, reg. no.121061500082-2).

**Conflict of interests:** The authors reported no potential conflict of interests.

## INTRODUCTION

Boreal forests play a crucial role in maintaining the Earth's ecological balance. As long-term carbon sinks, they mitigate the effects of climate change by reducing the concentration of greenhouse gases in the atmosphere. They also regulate the balance of water and heat, directly influencing regional and global climates (Bonan, 2008; IPCC, 2023; Gushchina et al., 2023; Olchev, 2025). Meanwhile, the current climate, characterized by rising global temperatures, changing precipitation patterns and higher frequency of regional hydrological and meteorological anomalies

(Mokhov, 2022), increases the risk of irreversible alteration in the structure and functions of forest ecosystems (Olchev et al., 2013; Groisman et al., 2017). Changes in the growth, productivity, and mortality of boreal tree species can affect taiga forests' ability to absorb carbon dioxide ( $\text{CO}_2$ ) from the atmosphere. It is crucial to understand and predict the consequences of climate change for deciduous and coniferous tree species because their capacity to absorb  $\text{CO}_2$  through photosynthesis directly impacts the global carbon cycle and the overall state of forest ecosystems (Tselniker et al., 1993; Molchanov, 2007; Suvorova & Popova, 2015; Olchev & Gulev, 2024).

Photosynthesis is the physiological basis of plant productivity. There are many mathematical models that describe photosynthesis at various scales, ranging from molecular interactions in thylakoid membranes to a whole plant or ecosystem (Laisk et al., 2009; Hikosaka et al., 2016; Sukhova et al., 2021). The Farquhar approach (Farquhar et al., 1980; von Caemmerer et al., 2000) is traditionally used to model net photosynthesis in tree leaves and ground vegetation. It has proven effective in predicting  $\text{CO}_2$  assimilation under various environmental conditions (Bernacchi et al., 2013; Busch et al., 2024; Stirbet et al., 2024). The model enables determining several key parameters, including the maximum carboxylation rate ( $V_{\text{C}}_{\text{max}}$ ), maximum rate of electron transport for the acceptor molecule ribulose 1,5-bisphosphate regeneration under saturating light ( $J_{\text{max}}$ ), triose phosphate utilization (TPU) rate, as well as dark respiration ( $R_d$ ) rate and mesophyll conductance ( $g_m$ ).

The parameters  $V_{\text{C}}_{\text{max}}$ ,  $J_{\text{max}}$ , and TPU are essential for modeling photosynthetic responses to environmental changes.  $V_{\text{C}}_{\text{max}}$  and  $J_{\text{max}}$  depend strongly on external conditions, particularly  $\text{CO}_2$  concentration and light intensity (Busch et al., 2024). Solar radiation directly impacts photosynthesis because it provides energy for electron transport and  $\text{CO}_2$  reduction. Light activation occurs through covalent and conformational modifications of enzymes that catalyze Calvin cycle reactions, particularly ribulose bisphosphate carboxylase/oxygenase (Rubisco) (Laisk et al., 2009). Light also influences  $\text{CO}_2$  diffusion between the air and the intercellular space of the leaf by regulating the width of the stomatal openings. An increase in air  $\text{CO}_2$  content contributes to enhanced Rubisco carboxylation activity (Norby et al., 2005). Electron transport is also sensitive to environmental factors as it depends on the stability of the thylakoid membrane (Hikosaka et al., 2016) and can vary widely even within a species (Bernacchi et al., 2013). The third parameter that limits photosynthesis is TPU, which is related to the export and utilization of triose phosphates. TPU reflects the capacity to synthesize starch in chloroplasts or export metabolites to the cytosol for sucrose synthesis (Sharkey, 2024). Sucrose is then transported through the phloem to the plant's heterotrophic tissues and organs. High rates of sucrose phosphate synthesis can deplete the pool of free inorganic phosphate, thereby limiting photophosphorylation (Sharkey, 1985; von Caemmerer, 2000). TPU primarily restricts photosynthetic carbon fixation under high  $\text{CO}_2$ , high light intensity, or low temperature (Bernacchi et al., 2013; Busch et al., 2024). The importance of assessing the temperature dependence of photosynthesis parameters is emphasized in the works of Medlyn et al. (2002), Lin et al. (2013), and Togashi et al. (2018). These parameters are crucial for predicting how vegetative cover will respond to the expected increase in air temperature and  $\text{CO}_2$  concentrations in the future.

Some studies have shown that photosynthetic parameters can vary depending on a plant's species or functional type (Medlyn et al., 2002; Lin et al., 2013). According to Wullschleger (1993) and Mandala et al. (2022), higher  $V_{\text{C}}_{\text{max}}$ ,  $J_{\text{max}}$ , and TPU values have been observed in annual herbaceous plants (75, 154, and 20  $\mu\text{mol m}^{-2} \text{s}^{-1}$ ) than in perennial woody species (44, 97, and 5  $\mu\text{mol m}^{-2} \text{s}^{-1}$ ). Interspecific differences in photosynthetic parameters have also been noted in forest tree species (Medlyn et al., 2002; Korzukhin & Tseleniker, 2009; Pridacha et al., 2022) and are associated with leaf mesostructure, growth, and development in different species during the growing season (Tseleniker et al., 1993; Oleksyn et al., 2000; Juárez-López et al., 2008).

The most common tree species in boreal forests belong to the genera *Pinus*, *Betula*, *Populus*, and *Alnus* (Afonin et al., 2008).

Despite occupying similar areas and having a wide ecological amplitude, boreal tree species, particularly *Pinus sylvestris* L., *Betula pendula* Roth, *Populus tremula* L., and *Alnus incana* (L.) Moench, exhibit noticeable ecophysiological differences. In a previous study, we examined how microclimatic and edaphic conditions of clear-cutting influence the functional characteristics of evergreen gymnosperm and deciduous angiosperm tree species. We identified species-specific changes in the photosynthetic water and nitrogen use efficiency and nutrient ratios in Scots pine, silver birch, aspen, and grey alder along the "clear-cut site – bilberry-type pine forest" gradient of environmental factors (Pridacha et al., 2021). The interspecific features of the consistency of xylem hydraulic characteristics and  $\text{CO}_2/\text{H}_2\text{O}$  gas exchange parameters in the leaves of the different species indicates that Scots pine and aspen have a more efficient and safer hydraulic structure as compared with silver birch (Pridacha et al., 2023). However, during a three-year observation period in the warm season, lower photosynthesis and dark respiration rates were obtained in Scots pine than in deciduous tree species (Pridacha & Semin, 2024).

Due to the low boreal tree species diversity, changes in  $\text{CO}_2$  gas exchange parameters of each species resulting from environmental disturbances and climate change can significantly affect the carbon budget of taiga forests (Kurepin et al., 2018; Dusenge et al., 2020; Gagné et al., 2020). However, despite the recognized importance of assessing photosynthesis parameters for modeling and predicting carbon fluxes in terrestrial ecosystems (Laisk et al., 2009; Hikosaka et al., 2016), the impact of environmental changes on these parameters is still not fully understood. To address the lack of knowledge in this area, we examined the effects of temperature on photosynthesis parameters in co-growing an evergreen gymnosperm (*Pinus sylvestris* L.) and three deciduous angiosperm (*Betula pendula* Roth, *Populus tremula* L., and *Alnus incana* (L.) Moench) tree species in a clear-cut of mid-taiga bilberry-type pine forest. The choice of experimental design was based on the fact that clear-cuts are an ideal subject for studying how plant communities respond to environmental changes because the processes occurring in them are primarily influenced by natural factors. The working hypothesis of the study was that different tree species that grow together would show similar responses to environmental changes in the European North. Analyzing the relationship between photosynthesis parameters and environmental factors helps us understand the mechanisms of plant adaptation in response to environmental changes, particularly in the context of climate change.

## MATERIALS AND METHODS

### Study area and tree-growing conditions

The study was carried out in July 2018 in the European part of the middle taiga forest zone (Republic of Karelia) on a 10-year-old, clear-cut of bilberry-type pine forest (62°10'28.1''N, 33°59'58.8''E). According to the Köppen climate classification system, the climate of the study area is humid continental with cool summers (Peel et al., 2007). The area is characterized by high relative humidity (averaging 75%) and significant precipitation throughout the year (550–750 mm), 350–400 mm of which falls during the snow-free period from May to October (Nazarova, 2021). According to the climatic means for the period from 1991 to 2020, the average annual air temperature is +3.6°C, with minimum and maximum values of –8.4°C and +17.1°C in January and July, respectively. The average air temperature during the growing season (May–September) is +13°C. The total radiation balance for the growing season is 1,130 MJ  $\text{m}^{-2}$ . According

to data from the Kondopoga weather station, the growing season from May to September of 2018 in the study area was relatively warm ( $0.7^{\circ}\text{C} < \Delta T_{\text{seas.}} < 3.0^{\circ}\text{C}$ ) and characterized by a precipitation deficiency relative to the long-term climatic mean in May, June, and July (44, 52, and 77% of the climatic means, respectively), followed by a rainy August (151% of the climatic mean).

The study examined 10-year-old Scots pine (*Pinus sylvestris* L.), silver birch (*Betula pendula* Roth), aspen (*Populus tremula* L.), and grey alder (*Alnus incana* (L.) Moench) trees growing in a clear-cut bilberry-type pine forest site. The young stand that formed through natural regeneration in the clear-cut are primarily Scots pine (70%), with a mix of silver birch and aspen trees. The understory consists of grey alder, willow, and rowan (Pridacha & Semin, 2024). Five model trees have been selected for each of the species in the clear-cut site. The highest recorded values for height and trunk diameter at the site were for grey alder ( $4.5 \pm 1.3$  m and  $4.3 \pm 1.7$  cm, respectively) and silver birch ( $3.4 \pm 0.2$  m and  $1.8 \pm 0.2$  cm, respectively). The lowest values were observed for Scots pine ( $2.3 \pm 0.1$  m and  $1.6 \pm 0.1$  cm, respectively) and aspen ( $1.8 \pm 0.5$  m and  $1.2 \pm 0.4$  cm, respectively) (Pridacha et al., 2021).

The soil in the site was an Arenic Albic Podzol. Roots were mostly concentrated within 2–25 cm depth. The ground water table depth was 1.2 m. The detailed characteristics of the vegetation and soil cover of the clear-cut site have been presented in previous studies (Pridacha et al., 2021; Pridacha & Semin, 2024).

### Parameters of $\text{CO}_2$ gas exchange

Field measurements of key photosynthetic parameters were conducted in July 2018 in the clear-cut bilberry pine forest site on the leaves of *B. pendula*, *P. tremula*, *A. incana* and on the 1-year-old needles of *P. sylvestris*. Measurements were taken during daylight hours from 10 a.m. to 4 p.m. on intact leaves in the middle part of the plant's crown. A portable photosynthetic system LI-6400XT (LI-COR Inc., USA) was used for the measurements. The system was equipped with a  $\text{CO}_2$  injector, a standard 2 cm  $\times$  3 cm leaf chamber, and a LI-6400-02B LED light source (LI-COR Inc., USA). Healthy, fully formed leaves without visible damage were sampled from all plants using a uniform method with three biological replicates for each species. All the experiments were conducted under similar weather conditions.

The photosynthesis measurement program involved obtaining light and carbon dioxide response curves for photosynthesis parameters at leaf (needle) surface temperatures ranging from  $20^{\circ}\text{C}$  to  $35^{\circ}\text{C}$ . Both response curves were measured separately at each leaf temperature (20, 25, 30, and  $35^{\circ}\text{C}$ ). The range of leaf temperatures was chosen based on the plant growth temperature ( $20^{\circ}\text{C}$ ), a reference temperature (usually  $25^{\circ}\text{C}$ ), and temperatures above  $20^{\circ}\text{C}$  ( $30$ – $35^{\circ}\text{C}$ ). The average leaf adaptation time to chamber conditions was about 15 minutes. The  $\text{CO}_2$  response function of  $\text{CO}_2$  gas exchange in leaves (A/Ci-curve) was determined by sequentially changing the  $\text{CO}_2$  concentration in the leaf chamber (400, 300, 200, 100, 60, 30, 400, 600, 800, 1000, 1200, and 1600  $\mu\text{mol CO}_2 \text{ mol}^{-1}$ ) at a saturating light intensity of 1600  $\mu\text{mol m}^{-2} \text{ s}^{-1}$ , in accordance with the device's standard configuration (Busch, 2024). A/Ci-curve measurements were also performed under lower light conditions (400 and 100  $\mu\text{mol m}^{-2} \text{ s}^{-1}$ ) in a leaf chamber at a leaf surface temperature of  $25^{\circ}\text{C}$ . The relative humidity in the measuring chamber was set to 50% to prevent stomatal closure during the measurements.

The light response of photosynthetic parameters (A/Q-curve) was determined by measuring the intensity of  $\text{CO}_2$  gas

exchange at various PAR values (1600, 1200, 900, 600, 300, 150, 100, 75, 50, 25, and 0  $\mu\text{mol m}^{-2} \text{ s}^{-1}$ ) under constant  $\text{CO}_2$  concentrations (400  $\mu\text{mol CO}_2 \text{ mol}^{-1}$ ) and relative air humidity (50%) in the leaf chamber. The A/Q-curve measurements were also performed at higher  $\text{CO}_2$  concentrations (800 and 1200  $\mu\text{mol CO}_2 \text{ mol}^{-1}$ ) and a leaf temperature of  $25^{\circ}\text{C}$ .

The  $\text{CO}_2$  response curves (A/Ci-curve) were used to calibrate the key parameters of the Farquhar photosynthesis model (Farquhar et al., 1980) as modified by Sharkey et al. (2007): maximum carboxylation rate ( $V_c^{\max}$ ), electron transport rate at light saturation ( $J_{\max}$ ), triose phosphate utilization rate ( $TPU$ ), and dark respiration rate ( $R_d$ ). The temperature dependencies of  $V_c^{\max}$ ,  $J_{\max}$ , and  $TPU$  were obtained by statistically evaluating a set of the photosynthesis parameter values at various leaf temperatures. Based on these dependencies, the standardized  $V_c^{\max25}$ ,  $J_{\max25}$ , and  $TPU_{25}$  values were obtained at the selected reference temperature of  $25^{\circ}\text{C}$  (Sharkey et al., 2007; Sharkey, 2016).

The parameters of the light response curve model, particularly the value of photosynthesis at saturating PAR values ( $A_{\max}$ ), were calculated using a modified Michaelis–Menten function (Kaipainen, 2009; Pridacha et al., 2022). Detailed procedures for assessing the carbon dioxide and light-response functions of  $\text{CO}_2$  gas exchange have been reported in previously published studies (Sharkey et al., 2007; Sharkey, 2016; Busch, 2024).

The  $\text{CO}_2$  gas exchange rates for *P. sylvestris* needles in our study were converted to the entire needle surface area. To calculate the surface area of the needles, we used a simplified method to determine their specific linear density (weight of unit needle length) (Tselniker, 1982).

### Statistical analysis

Statistical data analysis was performed using Statistica 13.3 (TIBCO Software Inc., USA). Regression analysis was used to process the experimental data. Statistical significance was defined as  $p < 0.05$ . The diagrams show the means and their standard errors.

## RESULTS

The classic biochemical Farquhar model and regression analysis of photosynthesis light response curves accurately describe how leaf photosynthesis responds to changes in ambient  $\text{CO}_2$  concentrations and light conditions, with an  $R^2$  value ranging from 0.95 to 0.99 (Fig. 1).

Analysis of the temperature dependence of photosynthetic parameters revealed that increasing leaf temperature within the  $20$ – $35^{\circ}\text{C}$  range resulted in 5.6- and 3.1-fold increases in  $V_c^{\max}$  in *P. sylvestris* and *B. pendula*, respectively (Fig. 2). In *A. incana* and *P. tremula*,  $V_c^{\max}$  increased within a narrower temperature range ( $20$ – $30^{\circ}\text{C}$ ) than in *P. sylvestris* and *B. pendula*. The increase was 2.2- and 3.1-fold, respectively, followed by a subsequent decrease of 1.2- and 2.1-fold at  $35^{\circ}\text{C}$  in *A. incana* and *P. tremula*, respectively. Analysis of the standardized  $V_c^{\max25}$  values at a reference temperature of  $25^{\circ}\text{C}$  revealed similar patterns of change for this parameter in each species. The  $V_c^{\max25}$  values were higher than the  $20^{\circ}\text{C}$  measured values (1.7-, 1.5-, 1.4-, and 1.5-fold for *P. sylvestris*, *B. pendula*, *A. incana*, and *P. tremula*, respectively) and lower at  $30^{\circ}\text{C}$  (1.4- to 1.6-fold) and  $35^{\circ}\text{C}$  (2- to 2.4-fold) for all species. At a leaf surface temperature of  $25^{\circ}\text{C}$ ,  $V_c^{\max}$  values were lowest for 1-year-old *P. sylvestris* needles ( $38.8 \mu\text{mol m}^{-2} \text{ s}^{-1}$ ) and highest for *B. pendula*, *A. incana*, and *P. tremula* leaves (93.5, 86.1, and  $58.6 \mu\text{mol m}^{-2} \text{ s}^{-1}$ , respectively).

The  $J_{\max}$  values for *P. sylvestris* increased 2.5-fold within the temperature range of  $20$ – $35^{\circ}\text{C}$ . However, the increase was

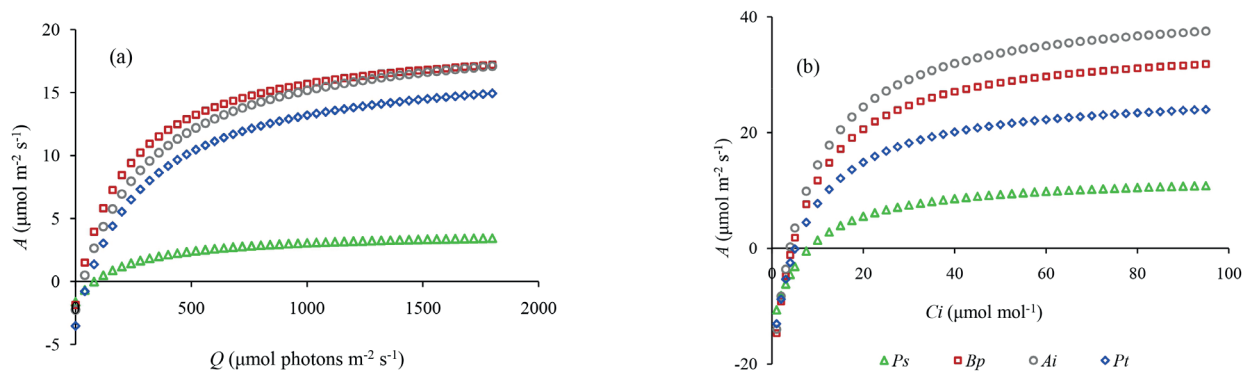


Fig. 1. Sample A/Q-curve (a) and A/Ci-curve (b) plotted for 1-year-old needles of *Pinus sylvestris* (*Ps*) and leaves of *Betula pendula* (*Bp*), *Alnus incana* (*Ai*), *Populus tremula* (*Pt*) at leaf temperature of 25°C using the LI-6400 XT protocol

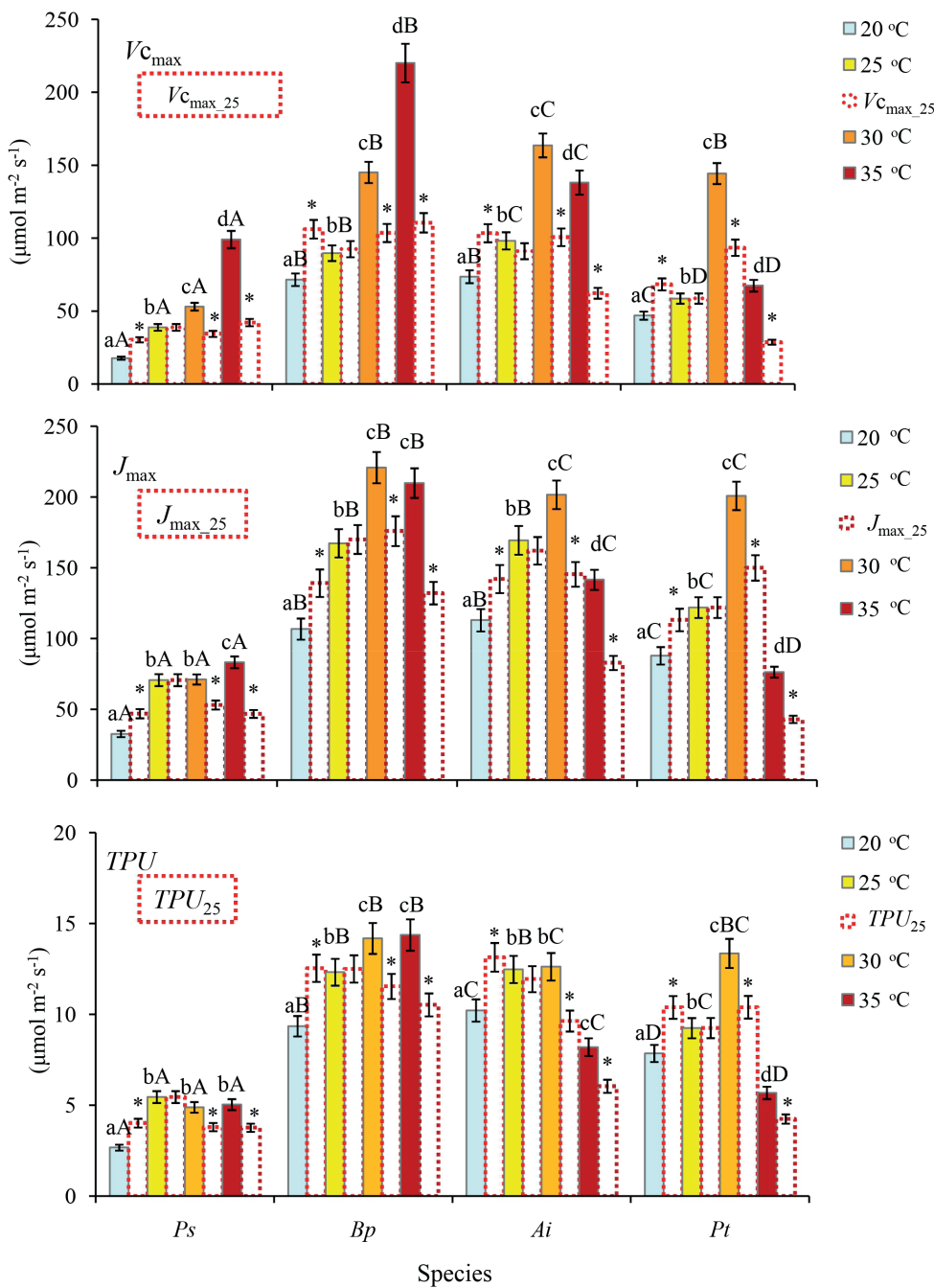


Fig. 2. Maximum rates of carboxylation by Rubisco ( $V_{C_{\max}}$ ), electron transport ( $J_{\max}$ ), and triose phosphate utilization ( $TPU$ ) measured in the leaf temperature range of 20–35°C and standardized at a reference temperature of 25°C ( $V_{C_{\max25}}$ ,  $J_{\max25}$ , and  $TPU_{25}$ ) in *Pinus sylvestris* (*Ps*), *Betula pendula* (*Bp*), *Alnus incana* (*Ai*), and *Populus tremula* (*Pt*). Different lowercase letters on top of the bars (a, b, c) indicate significant differences in means ( $p < 0.05$ ) when comparing one species at different leaf temperatures, and different capital letters (A, B, C) indicate significant differences ( $p < 0.05$ ) between different species at each treatment level. An asterisk (\*) indicates a significant difference in means ( $p < 0.05$ ) when comparing each pair of measured and standardized parameter values for each species

significantly lower, at only 1.2-fold, at temperatures between 25 and 35°C. For *B. pendula*, the  $J_{max}$  values increased 2-fold with an increase in leaf surface temperature from 20 to 35°C. For *A. incana* and *P. tremula*, this parameter increased up to 30°C (by 1.8 and 2.3 times, respectively) and then decreased at 35°C (by 1.4 and 2.6 times, respectively). Comparing the measured  $J_{max}$  values with the reference  $J_{max}$  values at 25°C revealed higher values for all species at 20°C (1.4, 1.3, 1.3, and 1.3 times higher for *P. sylvestris*, *B. pendula*, *A. incana*, and *P. tremula*, respectively). However, the corresponding values were lower at 30°C (by 1.3–1.4 times) and 35°C (by 1.6–1.8 times) in all species. The lowest  $J_{max25}$  values were observed for 1-year-old needles of *P. sylvestris* (70.7  $\mu\text{mol m}^{-2} \text{s}^{-1}$ ), compared to the deciduous species: 172.1, 155.1, and 122  $\mu\text{mol m}^{-2} \text{s}^{-1}$  for *B. pendula*, *A. incana*, and *P. tremula*, respectively.

As the temperature of the leaf surface raised from 20 to 35°C, the  $TPU$  values increased 1.9-fold in *P. sylvestris* trees and 1.5-fold in *B. pendula* trees. For *A. incana* and *P. tremula*, the  $TPU$  values increased 1.2- and 1.7-fold, respectively, when the leaf temperature increased from 20 to 30°C. Then, it decreased 1.5- and 2.4-fold, respectively, at 35°C. As with  $V_{C_{max}}$  and  $J_{max}$ , higher referenced  $TPU$  values were observed for all species at 20°C than the measured values (1.5, 1.3, 1.3, and 1.3 times higher for *P. sylvestris*, *B. pendula*, *A. incana*, and *P. tremula*, respectively). Lower values were observed at 30°C (1.2–1.3 times lower) and 35°C (1.3–1.4 times lower) in all species. 1-year-old needles of *P. sylvestris* had the lowest  $TPU_{25}$  values

(5.5  $\mu\text{mol m}^{-2} \text{s}^{-1}$ ) at a leaf temperature of 25°C compared to *B. pendula* (12.7  $\mu\text{mol m}^{-2} \text{s}^{-1}$ ), *A. incana* (11.4  $\mu\text{mol m}^{-2} \text{s}^{-1}$ ), and *P. tremula* (9.3  $\mu\text{mol m}^{-2} \text{s}^{-1}$ ) leaves.

Importantly, decreases in  $V_{C_{max}}$ ,  $J_{max}$ , and  $TPU$  values occurred when the light intensity in the leaf chamber decreased from saturating to low levels at a leaf surface temperature of 25°C for all tree species (Fig. 3). At the same time, interspecific differences in the dynamics of these parameters were revealed. For example, *P. sylvestris* showed the smallest decrease in  $V_{C_{max25}}$ ,  $J_{max25}$ , and  $TPU_{25}$  values (1.2-, 1.5-, and 1.5-fold, respectively) within the PAR range of 100 to 1,600  $\mu\text{mol m}^{-2} \text{s}^{-1}$  compared to deciduous species (3.1- to 3.2-, 4.3- to 4.8-, and 4.1- to 4.4-fold, respectively). Conversely, a 4-fold decrease in light intensity (from 1,600 to 400  $\mu\text{mol m}^{-2} \text{s}^{-1}$ ) led to a smaller decrease in  $V_{C_{max25}}$ ,  $J_{max25}$ , and  $TPU_{25}$  values in deciduous species (1.3–1.8, 1.4–1.6, and 1.4–1.6 times, respectively) than in *P. sylvestris* ( $J_{max25}$  and  $TPU_{25}$  by 1.3 times).

Analysis of  $A_{max}$  values revealed insignificant changes in *P. sylvestris*, *B. pendula*, and *A. incana* at leaf temperatures of 20–25°C, followed by a decrease in this parameter as the temperature increased to 35°C (decreasing by 1.9, 1.9, and 2.8 times, respectively) (Fig. 4a). *P. tremula* featured a greater stabilization of  $A_{max}$  in the 20–30°C range and a smaller decline in the parameter at 35°C (1.3 times) compared with other species. Increasing the  $\text{CO}_2$  concentration in the leaf chamber to 800 and 1,200  $\mu\text{mol CO}_2 \text{ mol}^{-1}$  for all tree species

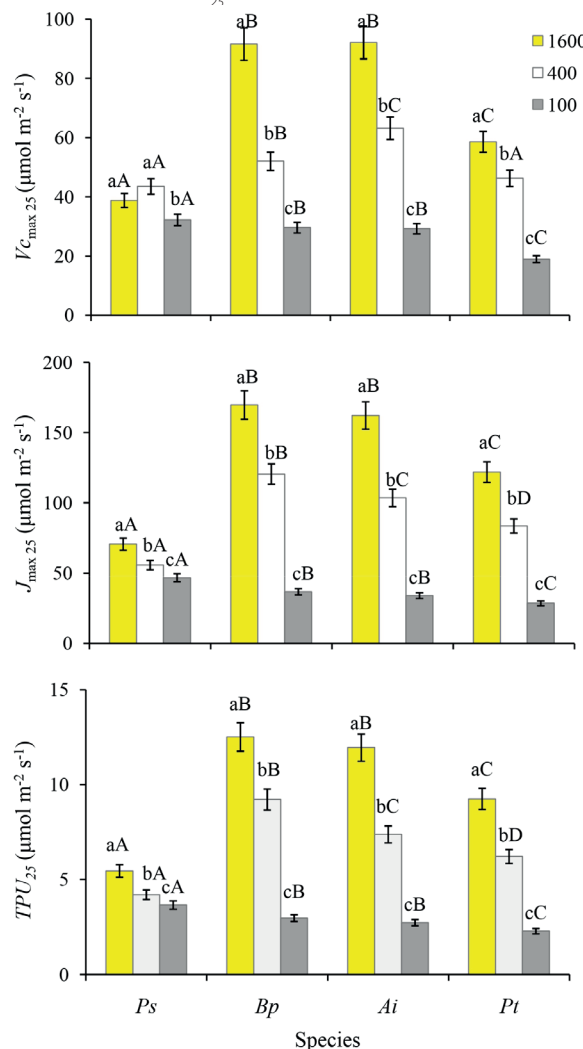


**Fig. 3. Maximum rates of carboxylation by Rubisco ( $V_{C_{max25}}$ ), electron transport ( $J_{max25}$ ), and triose phosphate utilization ( $TPU_{25}$ ) measured under different light intensities (100–1600  $\mu\text{mol m}^{-2} \text{s}^{-1}$ ) on 1-year-old needles of *Pinus sylvestris* (Ps) and leaves of *Betula pendula* (Bp), *Alnus incana* (Ai), and *Populus tremula* (Pt) at a leaf temperature of 25°C. Different lowercase letters on top of the bars (a, b, c) indicate significant differences in means ( $p < 0.05$ ) when comparing one species at different light intensity, and different capital letters (A, B, C) indicate significant differences ( $p < 0.05$ ) between different species at each light level.**

resulted in higher  $A_{max}$  values at a leaf surface temperature of 25°C (Fig. 4b). *P. sylvestris* exhibited the greatest increase in the parameter, with a 2- and 3-fold increase in CO<sub>2</sub> concentration relative to external conditions (1.9 and 2.6 times, respectively) compared to deciduous species, such as *P. tremula* (1.4 and 1.6 times, respectively), *B. pendula* (1.1 and 1.9 times, respectively), and *A. incana* (1.7 and 2.1 times, respectively).

Analysis of the temperature dependence of the  $J_{max}/Vc_{max}$  ratio, calculated from measured values between 20 and 35°C, revealed a negative linear relationship for all tree species (Fig. 5a). The decrease of the parameter with an increase in leaf temperature from 25 to 35°C was 2.2, 2.0, 1.7, and 1.8 times for

*P. sylvestris*, *B. pendula*, *A. incana*, and *P. tremula*, respectively. The  $J_{max25}/Vc_{max25}$  ratio, calculated using reference values at 25°C, exhibited similar dependence, taking the form of a "bell curve" with a pronounced peak at 25°C for all species studied (Fig. 5b). The increase in the  $J_{max25}/Vc_{max25}$  ratio in response to leaf temperature elevation in the 20–25°C range and its decline in the 25–35°C range were, respectively, 1.2 and 1.6-fold for *P. sylvestris* versus 1.3–1.4 and 1.4–1.5-fold for the deciduous species. It is also important to note the similarity of the  $J_{max25}/Vc_{max25}$  ratio at 25°C for *P. sylvestris*, *B. pendula*, and *A. incana* (1.8), as well as higher value for *P. tremula* (2.1).

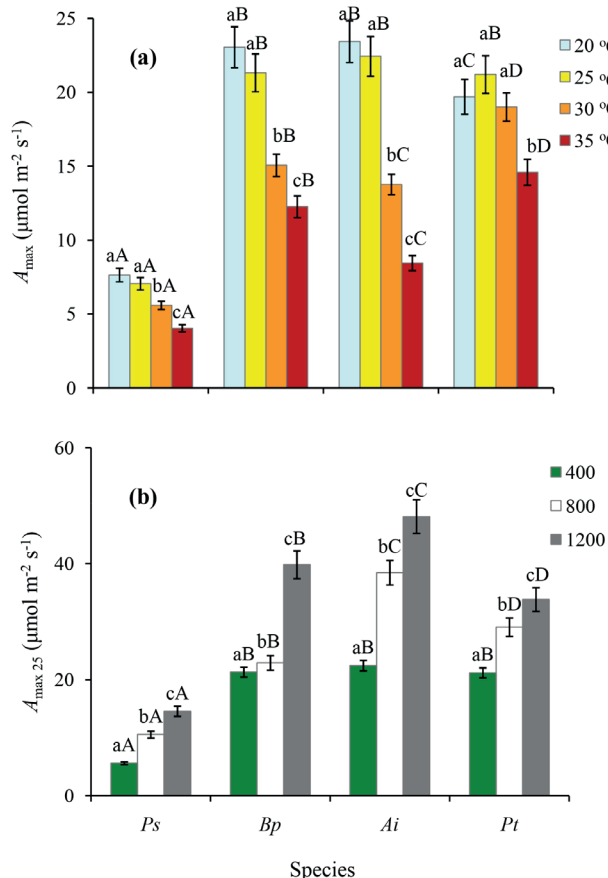


Fig. 4. Maximum CO<sub>2</sub> assimilation rate ( $A_{max}$ ) measured at leaf temperatures ranging from 20 to 35°C (a) and at different CO<sub>2</sub> concentrations ranging from 400 to 1200  $\mu\text{mol CO}_2 \text{ mol}^{-1}$  at a leaf temperature of 25°C (b) on 1-year-old needles of *Pinus sylvestris* (Ps) and leaves of *Betula pendula* (Bp), *Alnus incana* (Ai), and *Populus tremula* (Pt). Different lowercase letters on top of the bars (a, b, c) indicate significant differences in means ( $p < 0.05$ ) when comparing one species at different leaf temperatures or CO<sub>2</sub> concentrations, and different capital letters (A, B, C) indicate significant differences ( $p < 0.05$ ) between different species at each treatment level

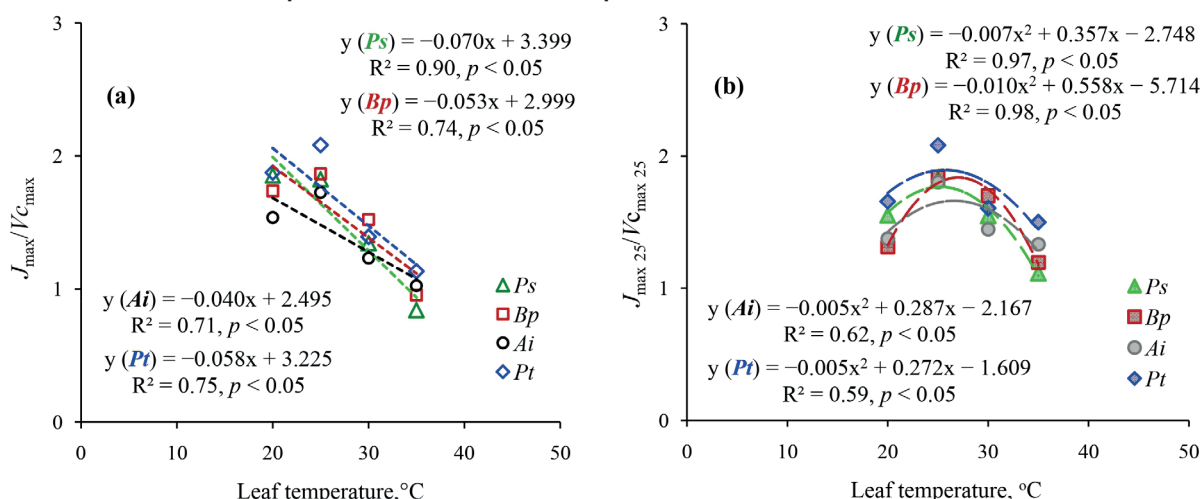


Fig. 5. Ratio of maximum electron transport rate ( $J_{max}$ ) and maximum rate of carboxylation by Rubisco ( $Vc_{max}$ ) measured at leaf temperature ranging from 20 to 35°C (a) and standardized at 25°C (b) in *Pinus sylvestris* (Ps), *Betula pendula* (Bp), *Alnus incana* (Ai) and *Populus tremula* (Pt)

## DISCUSSION

### Temperature dependence of photosynthesis parameters

The study examining the temperature dependence of photosynthetic parameters in four boreal tree species (*Pinus sylvestris*, *Betula pendula*, *Populus tremula*, and *Alnus incana*) revealed significant species-specific differences in the responses of  $V_{C_{max}}$ ,  $J_{max}$ , and  $TPU$  to changes in leaf temperature and light conditions. These results provide a deeper understanding of how trees in cold climates adapt to changing environmental conditions, particularly in the context of global climate change.

Analysis of the temperature dependence of photosynthetic parameters (Fig. 2) revealed that *P. sylvestris* and *B. pendula* exhibited the greatest increase in  $V_{C_{max}}$  with temperature increases from 20 to 35°C. In contrast, *A. incana* and *P. tremula* demonstrated a narrower optimal temperature range (20 to 30°C) and a subsequent decrease in  $V_{C_{max}}$  at 35°C compared to 30°C. These results agreed with previous studies suggesting that coniferous species, including *P. sylvestris*, exhibit a broader temperature range for photosynthesis than deciduous species (Medlyn et al., 2002; Lin et al., 2013). The decrease in  $V_{C_{max}}$  in deciduous species at high temperatures may be related to the temperature-dependent activity of Rubisco, the inactivation of Rubisco due to reduced functioning of Rubisco activase, or the decreased stability of the enzyme (Sharkey, 1985; Galmés et al., 2015; Scafaro et al., 2023).

Similarly,  $J_{max}$  increased gradually in *P. sylvestris* and *B. pendula*, whereas *A. incana* and *P. tremula* exhibited a sharp increase in  $J_{max}$ , followed by a decrease, at 35°C. These results suggest that deciduous species, particularly *A. incana* and *P. tremula*, have more sensitive electron transport systems to elevated temperatures. This is likely due to the destabilization of thylakoid membranes and their components (Hikosaka et al., 2016). These results align with data indicating that high temperatures, which frequently occur during summer heat waves, can significantly limit the functioning of boreal deciduous species (Reich et al., 2018; Dusenge et al., 2020).

The  $TPU$  (triose phosphate utilization) parameter exhibited less variability in *P. sylvestris* and *B. pendula* than in *A. incana* and *P. tremula* within a temperature range of 25–35°C. This suggests that these species use carbohydrates (triose phosphates) more efficiently for synthesizing sucrose and starch under thermal stress compared to *A. incana* and *P. tremula*. However, the decrease in  $TPU$  in deciduous species at 35°C may result from limitations in starch and sucrose synthesis or phosphate recycling (Sharkey, 1985; von Caemmerer, 2000; Hikosaka et al., 2016). These findings have significant implications for long-term carbon accumulation under warming conditions.

The decrease in  $A_{max}$  observed in all species (Fig. 4a) as the temperature increases beyond the optimal range is due to the fact that the rate at which plants absorb  $CO_2$  via photosynthesis is influenced by the photosynthetic apparatus and the degree of stomatal opening (Lin et al., 2012; Scafaro et al., 2023). Within the super-optimal temperature range, the decrease in photosynthetic intensity is due to a reduction in leaf turgor and stomatal closure. This hinders the diffusion of  $CO_2$  from the atmosphere into the interior of the leaf and to the fixation centers. Additionally, as temperature rises,  $CO_2$  solubility decreases, and the kinetic constants of carboxylating enzymes change (Sage & Kubien, 2007). As temperature increases, Rubisco's affinity for oxygen grows, enhancing photorespiration and reducing the efficiency of carbon dioxide fixation. This results in a decrease in the overall rate of photosynthesis.

It is important to note the greater thermal stability of  $A_{max}$  in *P. tremula* compared to other species across a broader temperature range (20–30°C), as well as the higher

$A_{max}$  values observed at sub-optimal temperatures (30–35°C). However, *P. tremula* exhibits lower photosynthetic activity than other deciduous species, as evidenced by lower  $V_{C_{max}}$ ,  $J_{max}$ , and  $TPU$  values. Our observations align with prior research indicating that biochemical factors and mesophyll limitations primarily drive the decrease in photosynthesis in *P. tremula* at high temperatures and  $CO_2$  concentrations (Hüve et al., 2019; de Souza et al., 2024). During four growing seasons at the same clear-cut site, we observed higher values of stomatal conductance and transpiration rate for *P. tremula* than for other deciduous species and *P. sylvestris* (Pridacha et al., 2021). These findings are important because stomatal conductance determines the rate of  $CO_2$  diffusion to carboxylation sites (Baillie, Fleming, 2020; Márquez, Busch, 2024), and transpiration provides leaf thermoregulation by evaporating water from the leaf surface. This cooling effect prevents overheating, especially at high ambient temperatures (Lin et al., 2017; Drake et al., 2018). Thus, the greater thermal stability of  $A_{max}$  in *P. tremula* relative to other species can be due to higher  $CO_2$  diffusion flux and better leaf thermoregulation. This is consistent with noted relative independence of  $CO_2$  concentration in *P. tremula* leaf chloroplasts from temperature (de Souza et al., 2024).

Additionally, the greater thermal stability range of  $A_{max}$  in *P. tremula* may be due to differences in hydraulic regulation among species, specifically the anisohydric nature of *P. tremula* compared to the isohydric characteristics of *B. pendula* (Pridacha et al., 2023). This hypothesis is supported by data from other studies (Klein, 2014; Meinzer et al., 2016; Sellin et al., 2019, 2022). A previous study (Mäenpää et al., 2011) on the effects of ozone and temperature on carbon assimilation in *B. pendula* and *P. tremula* seedlings found that *B. pendula* leaves experienced a greater decrease in stomatal conductance (1.7 times) than *P. tremula* leaves (1.2 times) when the air temperature increased by 1°C. This is consistent with the more pronounced decrease in  $A_{max}$  in *B. pendula* with an increase in temperature above the optimum relative to *P. tremula* (Fig. 4a). This is likely because of a greater decrease in  $CO_2$  diffusion flux into the leaf due to stomatal limitation of photosynthesis, despite higher activity of the photosynthetic apparatus in *B. pendula* (Fig. 2).

At the same time, in all species we observed a similar consistent pattern of the  $J_{max}/V_{C_{max}}$  ratio at temperatures between 20 and 25°C, which decreased as the temperature increased up to 35°C (Fig. 5). Despite interspecific differences, this pattern can be explained by the optimal temperature range for photosynthesis in  $C_3$  plants, which is typically between 20–25 °C for most  $C_3$  plants in the temperate zone (Laisk et al., 2009; Hikosaka et al., 2016). The decrease in the  $J_{max}/V_{C_{max}}$  ratio from 1.7–2.1 to 0.8–1.1 with increasing temperature for all species may be associated with the higher activation energy for  $V_{C_{max}}$  relative to  $J_{max}$ . Similar observations have been made by scientists studying other woody plants (Onoda et al., 2005; Ow et al., 2008; Riikonen et al., 2009). The similarity of the Rubisco specificity factor in gymnosperms and  $C_3$  angiosperms has also been noted, as a measure of the enzyme's capacity to exhibit carboxylase and oxygenase activity relative to RubP. This similarity is explained by the adaptation of Rubisco in different phylogenetic groups of plants to current  $CO_2/O_2$  atmospheric levels (Miyazawa et al., 2020).

### Response to light and $CO_2$

The study also revealed interspecific differences in photosynthetic responses to changes in light intensity and  $CO_2$  levels. *P. sylvestris* exhibited greater stability in  $V_{C_{max}}$  and

$J_{max}$  at low light levels ( $100\text{--}400 \mu\text{mol m}^{-2} \text{s}^{-1}$ ). In contrast, deciduous species demonstrated a more significant decline in these parameters (Fig. 3). This may reflect conifers' adaptation to shading or high cloud cover in boreal regions (Oleksyn et al., 1998; Ma et al., 2014; Schmiege et al., 2023). Due to their higher photosynthetic activity, deciduous trees likely experience more pronounced inhibition of Rubisco activity at low light levels due to the strong binding of RuBP and other sugar phosphates formed during the Calvin cycle to the catalytic center (Sharkey, 1985; von Caemmerer, 2000).

At elevated  $\text{CO}_2$  concentrations ( $800\text{--}1200 \mu\text{mol mol}^{-1}$ ), the greatest increase in  $A_{max}$  was observed in *P. sylvestris* (Fig. 4b), suggesting a stronger response to  $\text{CO}_2$  enrichment than in deciduous species. These results are consistent with previous studies (Niinemets et al., 2011; Kurepin et al., 2018) that reported conifers' superior adaptation to elevated  $\text{CO}_2$  levels. Since  $\text{CO}_2$  is a substrate for photosynthesis, its availability and concentration determine the activity of carbon metabolism. The increase in photosynthesis rate with increasing  $\text{CO}_2$  levels is due to the realization of the carboxylase potential of Rubisco and the formation of a large RuBP acceptor pool in chloroplasts under these conditions (von Caemmerer, 2000; Busch et al., 2024). Among the deciduous species, the greatest increase in  $A_{max}$  with  $\text{CO}_2$  growth was found in *A. incana*. We previously observed the highest values of specific nitrogen content and its biological absorption coefficient in *A. incana* relative to other species using the same model trees in the clear-cut (Pridacha et al., 2021). These results are consistent with previous studies reporting that trees of the genus *Alnus* can maintain high levels of photosynthesis after prolonged exposure to elevated  $\text{CO}_2$  in nitrogen-poor soils due to high nitrogen availability from symbiosis with nitrogen-fixing actinomycetes (Vogel, Curtis, 1995; Rytter, Rytter, 2016). However, the weak response of *P. tremula* to increased  $\text{CO}_2$  may indicate Rubisco activity saturation due to a greater supply of substrate ( $\text{CO}_2$ ) in the leaf caused by the higher stomatal conductance of *P. tremula* leaves (Pridacha et al., 2021) or limitations in subsequent metabolic processes (Busch et al., 2024).

It is important to note that the influence of mesophyll conductance on photosynthesis has been demonstrated for all plant functional types (Flexas et al., 2014; Nadal et al., 2021; Knauer et al., 2022). In our study, coniferous species exhibited the lowest photosynthesis parameter values under all temperature, light, and  $\text{CO}_2$  treatments compared to deciduous species. This finding aligns with prior studies indicating lower mesophyll conductance in coniferous trees than in deciduous trees, primarily due to the structural organization of their rigid leaves. Specifically, needles have thick mesophyll cell walls and chloroplasts, as well as a low ratio of chloroplast surface area to intercellular space per unit of leaf surface area (Veromann-Jürgenson et al., 2017; Carriqué et al., 2020). The low photosynthesis rates in coniferous trees are believed to be offset by their significantly longer active photosynthesis duration compared to deciduous trees in the boreal zone (Vasfilov, 2016; Shiklomanov et al., 2020). As temperatures and  $\text{CO}_2$  levels in the atmosphere rise in a changing climate, it is assumed that species with low mesophyll conductance, particularly evergreen gymnosperm, will gain an advantage over deciduous angiosperm tree species in terms of distribution, especially in the boreal zone (Niinemets et al., 2011; Flexas et al., 2014; Nadal et al., 2021).

The results of our study are consistent with previously published data, while also revealing some new findings. For example, Medlyn et al. (2002) observed similar  $Vc_{max}$  values for *P. sylvestris* at  $25^\circ\text{C}$ . However, our data show that this parameter is more sensitive to extreme temperatures. The decrease in

$J_{max}$  in deciduous species at  $35^\circ\text{C}$  aligns with results obtained for temperate forest species (Togashi et al., 2018; de Souza et al., 2024), suggesting stability in photosynthetic temperature sensitivity across different plant biomes. Differences in  $TPU$  among species are consistent with Wullschleger's (1993) data, which showed lower  $TPU$  values in woody perennials than in herbaceous plants. Our study extends these findings by demonstrating how these differences manifest with changes in temperature and light intensity.

The results highlight the vulnerability of boreal deciduous species, especially *A. incana* and *P. tremula*, to climate warming due to decreased photosynthetic efficiency at high temperatures. At the same time, all species exhibit a similar consistent pattern of the  $J_{max}/Vc_{max}$  ratio within the  $20\text{--}35^\circ\text{C}$  temperature range. However, *P. sylvestris* demonstrates greater resilience, confirming its dominant role in boreal forests under future warming conditions (Bonan, 2008). Nevertheless, the stronger response of coniferous species to elevated  $\text{CO}_2$  could be counterbalanced by other environmental stressors, such as drought. These factors were not considered in this study, yet they play a significant role in boreal ecosystem functioning (Reich et al., 2018; Liu et al., 2023; Martínez-García et al., 2024).

When considering the limitations of the identified patterns and prospects for future research, it should be noted that our study was conducted on young trees in a clear-cut area. This may not accurately reflect the functioning of a mature forest. Future studies should include mature trees and additional stress factors, such as drought and nutrient deficiency. Incorporating the data into ecosystem models based on the Farquhar approach will also improve predictions of the carbon cycle in boreal forests under climate change (Bernacchi et al., 2013).

## CONCLUSIONS

Our study of the temperature dependence of photosynthetic parameters in four boreal tree species (*Pinus sylvestris*, *Betula pendula*, *Populus tremula*, and *Alnus incana*) revealed significant differences in their adaptation strategies to changing environmental conditions. *P. sylvestris* and *B. pendula* had a broader optimal temperature range for  $J_{max}$  and  $Vc_{max}$  ( $20\text{--}35^\circ\text{C}$ ), whereas *P. tremula* and *A. incana* had optimal values between  $20$  and  $30^\circ\text{C}$  and experienced a sharp decline at  $35^\circ\text{C}$  compared to  $30^\circ\text{C}$ . These results indicate their greater vulnerability to increased temperatures and global warming. Additionally, *P. sylvestris* showed greater resilience in photosynthetic parameters under low light conditions, as well as a more pronounced response to elevated  $\text{CO}_2$  concentrations compared to deciduous species. This suggests its greater potential to adapt to future climate changes. The sensitivity of deciduous angiosperm tree species to extreme temperatures and increased  $\text{CO}_2$  levels could lead to shifts in the composition of boreal forests in the future.

The results obtained are important for predicting the carbon balance of boreal ecosystems. The resilience of *P. sylvestris* to high temperatures and its efficiency in using  $\text{CO}_2$  suggest that this species will maintain its dominant role in the warming climate. However, the vulnerability of deciduous angiosperm tree species requires further study, especially when considering additional stress factors such as drought. Integrating these data into the Farquhar approach-based ecosystem models will improve predictions of forest responses to climate change. Further studies should incorporate mature trees and complex stress scenarios to improve our understanding of the adaptive mechanisms of boreal species. ■

## REFERENCES

Afonin A.N., Greene S.L., Dzyubenko N.I., Frolov A.N. (eds.). (2008). Interactive agricultural ecological atlas of Russia and neighboring countries. Economic plants and their diseases, pests and weeds [Online]. Available at: <https://agroatlas.ru>.

Baillie A.L., Fleming A.J. (2020). The developmental relationship between stomata and mesophyll airspace. *New Phytol*, 225(3), 1120–1126. DOI: 10.1111/nph.16341

Bernacchi C.J., Bagley J.E., Serbin S.P., Ruiz-Vera U.M., Rosenthal D.M., Vanloocke A. (2013). Modelling  $C_3$  photosynthesis from the chloroplast to the ecosystem. *Plant Cell Environ*, 36(9), 1641–1657. DOI: 10.1111/pce.12118

Bonan G.B. (2008). Forests and climate change: forcings, feedbacks, and the climate benefits of forests. *Science*, 320, 1444–1449. DOI: 10.1126/science.1155121

Busch F.A. (2024). Photosynthetic gas exchange in land plants at the leaf level. In: Covshoff, S. (eds) *Photosynthesis. Methods in molecular biology*. V. 2790. Humana, New York, NY. DOI: 10.1007/978-1-0716-3790-6\_3

Busch F.A., Ainsworth E.A., Amtmann A., Cavanagh A.P., Driever S.M., Ferguson J.N., Kromdijk J., Lawson T., Leakey A.D., Matthews J.S., Meacham-Hensold K., Vath R.L., Vlaet-Chabrand S., Walker B.J., Papanatsiou M. (2024). A guide to photosynthetic gas exchange measurements: Fundamental principles, best practice and potential pitfalls. *Plant Cell Environ*, 47, 3344–3364. DOI: 10.1111/pce.14815

Carriquí M., Nadal M., Clemente-Moreno M.J., Gago J., Miedes E., Flexas J. (2020). Cell wall composition strongly influences mesophyll conductance in gymnosperms. *Plant J*, 103, 1372–1385. DOI: 10.1111/tpj.14806

de Souza V.F., Rasulov B., Talets E., Morfopoulos C., Albuquerque P.M., Junior S.D., Niinemets U., Goncales J.F. (2024). Thermal sensitivity determines the effect of high  $CO_2$  on carbon uptake in *Populus tremula* and *Inga edulis*. *Theor Exp Plant Physiol*, 36, 199–213. DOI: 10.1007/s40626-024-00312-9

Drake J.E., Tjoelker M.G., Vårhammar A., Medlyn B.E., Reich P.B., Leigh A., Pfautsch S., Blackman C.J., López R., Aspinwall M.J., Crous K.Y., Duursma R.A., Kumarathunge D., De Kauwe M.G., Jiang M., Nicotra A.B., Tissue D.T., Choat B., Atkin O.K., Barton C.V. (2018). Trees tolerate an extreme heatwave via sustained transpirational cooling and increased leaf thermal tolerance. *Glob Change Biol*, 24, 2390–2402. DOI: 10.1111/gcb.14037

Dusenge M.E., Madhavji S., Way D.A. (2020). Contrasting acclimation responses to elevated  $CO_2$  and warming between an evergreen and a deciduous boreal conifer. *Glob Change Biol*, 26, 3639–3657. DOI: 10.1111/gcb.15084

Farquhar G.D., von Caemmerer S., Berry J.A. (1980). A biochemical model of photosynthetic  $CO_2$  assimilation in leaves of  $C_3$  plants. *Planta*, 149, 78–90.

Flexas J., Carriquí M., Coopman R.E., Gago J., Galmés J., Martorell S., Morales F., Diaz-Espejo A. (2014). Stomatal and mesophyll conductances to  $CO_2$  in different plant groups: underrated factors for predicting leaf photosynthesis responses to climate change? *Plant Sci*, 226, 41–48. DOI: 10.1016/j.plantsci.2014.06.011

Gagne M.A., Smith D.D., McCullough K.A. (2020). Limited physiological acclimation to recurrent heatwaves in two boreal tree species. *Tree Physiol*, 40(12), 1680–1696. DOI: 10.1093/treephys/tpaa102

Galmés J., Kapralov M.V., Copolovici L.O., Hermida-Carrera C., Niinemets Ü. (2015). Temperature responses of the Rubisco maximum carboxylase activity across domains of life: phylogenetic signals, trade-offs, and importance for carbon gain. *Photosynth Res*, 123, 183–201. DOI: 10.1007/s11120-014-0067-8

Groisman P., Shugart H., Kicklighter D. et al. (2017). Northern Eurasia Future Initiative (NEFI): facing the challenges and pathways of global change in the twenty-first century. *Prog Earth Planet Sci*, 41. DOI: 10.1186/s40645-017-0154-5

Gushchina D., Tarasova M., Satosina E., Zheleznova I., Emelianova E., Gibadullin R., Osipov A., Olchev A. (2023). The response of daily carbon dioxide and water vapor fluxes to temperature and precipitation extremes in temperate and boreal forests. *Climate*, 11(10), 206. DOI: 10.3390/cli11100206

Hikosaka K., Niinemets Ü., Anten N.P. (eds.). (2016). *Canopy photosynthesis: from basics to applications. Advances in photosynthesis and respiration*. Vol. 42. Springer Dordrecht, 428 p. DOI: 10.1007/978-94-017-7291-4

Hüve K., Bichele I., Kaldmäe H., Rasulov B., Valladares F., Niinemets Ü. (2019). Responses of aspen leaves to heatflecks: both damaging and non-damaging rapid temperature excursions reduce photosynthesis. *Plants*, 8(6), 145. DOI: 10.3390/plants8060145

IPCC: Climate Change 2023: Synthesis Report, Summary for Policymakers. Contribution of Working Groups I, II and III to the Sixth Assessment Report of the Intergovernmental Panel on Climate Change. (2023). IPCC, Geneva, Switzerland, 34 p. DOI: 10.59327/IPCC/AR6-9789291691647.001

Juárez-López F.J., Escudero A., Mediavilla S. (2008). Ontogenetic changes in stomatal and biochemical limitations to photosynthesis of two co-occurring Mediterranean oaks differing in leaf life span. *Tree Physiol*, 28, 367–374. DOI: 10.1093/treephys/28.3.367

Kaipainen E.L. (2009). Parameters of photosynthesis light curve in *Salix dasyclados* and their changes during the growth season. *Russ J Plant Physiol*, 56, 445–453. DOI: 10.1134/S1021443709040025.

Klein T. (2014). The variability of stomatal sensitivity to leaf water potential across tree species indicates a continuum between isohydric and anisohydric behaviours. *Funct Ecol*, 28, 1313–1320. DOI: 10.1111/1365-2435.12289

Knauer J., Cuntz M., Evans J.R., Niinemets Ü., Tøsens T., Veromann-Jürgenson L.-L., Werner C., Zaehle S. (2022). Contrasting anatomical and biochemical controls on mesophyll conductance across plant functional types. *New Phytol*, 236, 357–368. DOI: 10.1111/nph.18363

Korzukhin M.D., Tselnicker Y.L. (2009). Analysis of the distribution and net primary production of four forest tree species in Russia using an ecophysiological model. In: *Problems of ecological monitoring and ecosystem modeling*, 22, 92–123.

Kurepin L.V., Stangl Z.R., Ivanov A.G., Bui V., Mema M., Hüner N.P., Öquist G., Way D., Hurry V. (2018). Contrasting acclimation abilities of two dominant boreal conifers to elevated  $CO_2$  and temperature. *Plant Cell Environ*, 41, 1331–1345. DOI: 10.1111/pce.13158

Laisk A., Nedbal L., Govindjee G. (eds.). (2009). *Photosynthesis in silico: understanding complexity from molecules to ecosystems. Advances in photosynthesis and respiration*. Vol. 29. Springer Dordrecht, 503p. DOI: 10.1007/978-1-4020-9237-4

Lin H., Chen Y., Zhang H., Fu P., Fan Z. (2017). Stronger cooling effects of transpiration and leaf physical traits of plants from a hot dry habitat than from a hot wet habitat. *Funct Ecol*, 31, 2202–2211. DOI: 10.1111/1365-2435.12923

Lin Y.-S., Medlyn B.E., Ellsworth D.S. (2012). Temperature responses of leaf net photosynthesis: the role of component processes. *Tree Physiol*, 32(2), 219–231. DOI: 10.1093/treephys/tpr141

Lin Y.-S., Medlyn B.E., Kauwe M.G., Ellsworth D.S. (2013). Biochemical photosynthetic responses to temperature: how do interspecific differences compare with seasonal shifts? *Tree Physiol*, 33(8), 793–806. DOI: 10.1093/treephys/tpt047

Liu Q., Peng C., Schneider R., Cyr D., McDowell N.G., Kneeshaw D. (2023). Drought-induced increase in tree mortality and corresponding decrease in the carbon sink capacity of Canada's boreal forests from 1970 to 2020. *Glob Change Biol*, 29, 2274–2285. DOI: 10.1111/gcb.16599

Ma Z., Behling S., Ford E.D. (2014). The contribution of dynamic changes in photosynthesis to shade tolerance of two conifer species. *Tree Physiol*, 34(7), 730–743. DOI: 10.1093/treephys/tpu054

Mäenpää M., Riikonen J., Kontunen-Soppela S., Rousi M., Oksanen E. (2011). Vertical profiles reveal impact of ozone and temperature on carbon assimilation of *Betula pendula* and *Populus tremula*. *Tree Physiol.*, 31, 819–830. DOI: 10.1093/treephys/tpr075

Márquez D.A., Busch F.A. (2024). The interplay of short-term mesophyll and stomatal conductance responses under variable environmental conditions. *Plant Cell Environ.*, 47, 3393–3410. DOI: 10.1111/pce.14880

Martínez-García E., Nilsson M.B., Laudon H., Lundmark T., Fransson J.E.S., Wallerman J., Peichl M. (2024). Drought response of the boreal forest carbon sink is driven by understorey–tree composition. *Nat Geosci.*, 17, 197–204. DOI: 10.1038/s41561-024-01374-9

Medlyn B.E., Dreyer E., Ellsworth D., Forstreuter M., Harley P.C., Kirschbaum M.U., Le Roux X., Montpied P., Strassemeyer J., Walcroft A., Wang K., Loustau D. (2002). Temperature response of parameters of a biochemically based model of photosynthesis. II. A review of experimental data. *Plant Cell Environ.*, 25, 1167–1179. DOI: 10.1046/j.1365-3040.2002.00891.x

Meinzer F.C., Woodruff D.R., Marias D.E., Smith D.D., McCulloh K.A., Howard A.R., Magedman A.L. (2016). Mapping 'hydroscapes' along the iso- to anisohydric continuum of stomatal regulation of plant water status. *Ecol Lett.*, 19, 1343–1352. DOI: 10.1111/ele.12670

Miyazawa S.I., Tobita H., Ujino-Ihara T., Suzuki Y. (2020). Oxygen response of leaf  $\text{CO}_2$  compensation points used to determine Rubisco specificity factors of gymnosperm species. *J Plant Res.*, 133, 205–215. DOI: 10.1007/s10265-020-01169-0

Mndela M., Tjelele J.T., Madakadze I.C., Mangwana M., Samuels I.M., Muller F., Pule H.T. (2022). A global meta-analysis of woody plant responses to elevated  $\text{CO}_2$ : implications on biomass, growth, leaf N content, photosynthesis and water relations. *Ecological Processes*, 11, 52–73. DOI: 10.1186/s13717-022-00397-7

Mokhov I.I. (2022). Climate change: causes, risks, consequences, and problems of adaptation and regulation. *Herald Russ Academy Sci.*, 92(1), 3–14. DOI: 10.31857/S0869587322010066.

Molchanov A.G. (2007).  $\text{CO}_2$  balance in ecosystems of pine and oak forests in different forest vegetation zones. Tula, 284 p.

Nadal M., Carriquí M., Flexas J. (2021). Mesophyll conductance to  $\text{CO}_2$  diffusion in a climate change scenario: effects of elevated  $\text{CO}_2$ , temperature and water stress. In: Becklin K.M., Ward J.K., Way D.A. (eds) *Photosynthesis, respiration, and climate change. Advances in photosynthesis and respiration*, 48. Springer, Cham. DOI: 10.1007/978-3-030-64926-5\_3

Nazarova L.E. (2021). Climatic conditions in the Republic of Karelia. In: *Current conditions of water basins of the North*. Petrozavodsk, 7–16 (In Russian).

Ninemets Ü., Flexas J., Peñuelas J. (2011). Evergreens favored by higher responsiveness to increased  $\text{CO}_2$ . *Trends Ecol Evol.*, 26(3), 136–142. DOI: 10.1016/j.tree.2010.12.012

Norby R.J., Delucia E.H., Gielen B., et al. (2005). Forest response to elevated  $\text{CO}_2$  is conserved across a broad range of productivity. *Proc Natl Acad Sci USA*, 102 (50), 18052–18056. DOI: 10.1073/pnas.0509478102

Olchev A.V., Deshcherevskaya O.A., Kurbatova Y.A., Molchanov A.G., Novenko E.Y., Pridacha V.B., Sazonova T.A. (2013).  $\text{CO}_2$  and  $\text{H}_2\text{O}$  exchange in the forest ecosystems of southern taiga under climate change. *Doklady Biol Sci.*, 450(1), 173–176. DOI: 10.1134/S0012496613030216

Olchev A.V., Gulev S.K. (2024). Carbon flux measurement supersites of the Russian Federation: objectives, methodology, prospects. *Izv Atmos Ocean Phys.*, 60 (Suppl 3), S428–S434. DOI: 10.1134/S0001433824700841

Olchev A.V. (2025). Estimation of carbon dioxide and methane emissions and absorption by land and ocean surfaces in the 21st century. *Izv Atmos Ocean Phys.*, 61 (Suppl 1), S74–S100. DOI: 10.1134/S0001433825701166

Oleksyn J., Modrzynski J., Tjoelker M.G., Zytkowiak R., Reich P.B., Karolewski P. (1998). Growth and physiology of *Picea abies* populations from elevational transects: common garden evidence for altitudinal ecotypes and cold adaptation. *Funct Ecol.*, 12, 573–590.

Oleksyn J., Zytkowiak R., Reich P.B., Tjoelker M.G., Karolewski P. (2000). Ontogenetic patterns of leaf  $\text{CO}_2$  exchange, morphology and chemistry in *Betula pendula* trees. *Trees*, 14, 271–281. DOI: 10.1007/PL00009768

Onoda Y., Hikosaka K., Hirose T. (2005). The balance between RuBP carboxylation and RuBP regeneration: a mechanism underlying the interspecific variation in acclimation of photosynthesis to seasonal change in temperature. *Funct Plant Biol.*, 32, 903–910. DOI: 10.1071/FP05024

Ow L.F., Griffin K.L., Whitehead D., Walcroft A.S., Turnbull M.H. (2008). Thermal acclimation of leaf respiration but not photosynthesis in *Populus deltoides* *x* *nigra*. *New Phytol.*, 178, 123–134. DOI: 10.1111/j.1469-8137.2007.02357.x

Peel M.C., Finlayson B.L., McMahon T.A. (2007). Updated world map of Köppen-Geiger climate classification. *Hydrol Earth Syst Sci.*, 11, 1633–1644. DOI: 10.5194/hess-11-1633-2007

Pridacha V.B., Makhmudova L.Sh., Semin D.E., Olchev A.V. (2022). Photosynthetic parameters of woody plant species in the foothills of northern Caucasian broadleaved forests. *Grozny Natural Science Bulletin*, 4(30), 105–112 (in Russian with English summary). DOI: 10.25744/genb.2022.74.70.009

Pridacha V.B., Sazonova T.A., Novichonok E.V., Semin D.E., Tkachenko Yu.N., Pekkoev A.N., Timofeeva V.V., Bakhmet O.N., Olchev A.V. (2021). Clear-cutting impacts nutrient, carbon and water exchange parameters in woody plants in an east Fennoscandian pine forest. *Plant Soil*, 466, 317–336. DOI: 10.1007/s11104-021-05058-w

Pridacha V.B., Semin D.E. (2024). Clear-cutting effects on components of the carbon balance in a bilberry-type pine forest in southern Karelia. *Ecosystem Transformation*, 7(3), 64–83. DOI: 10.23859/estr-230505

Pridacha V.B., Tarelkina T.V., Neronova Ya.A., Tumanik N.V. (2023). Significance of coordination between stem xylem traits and leaf gas exchange parameters during adaptation formation in some boreal species of Karelia. *Botanicheskii Zhurnal*, 108(7), 690–708. DOI: 10.31857/S000681362306008X

Reich P.B., Sendall K.M., Stefanski A., Rich R.L., Hobbie S.E., Montgomery R.A. (2018). Effects of climate warming on photosynthesis in boreal tree species depend on soil moisture. *Nature*, 562, 263–267. DOI: 10.1038/s41586-018-0582-4

Riikonen J., Mäenpää M., Alavillamo M., Silfver T., Oksanen E. (2009). Interactive effect of elevated temperature and  $\text{O}_3$  on antioxidant capacity and gas exchange in *Betula pendula* saplings. *Planta*, 230, 419–427. DOI: 10.1007/s00425-009-0957-8

Rytter L., Rytter R.-M. (2016). Growth and carbon capture of grey alder (*Alnus incana* (L.) Moench) under north European conditions – estimates based on reported research. *Forest Ecol Manag*, 2016, 373, 56–65. DOI: 10.1016/j.foreco.2016.04.034

Sage R.F., Kubien D.S. (2007). The temperature response of  $\text{C}_3$  and  $\text{C}_4$  photosynthesis. *Plant Cell Environ.*, 30, 1086–1106. DOI: 10.1111/j.1365-3040.2007.01682.x

Scafaro A.P., Posch B.C., Evans J.R., Farquhar G.D., Atkin O.K. (2023). Rubisco deactivation and chloroplast electron transport rates co-limit photosynthesis above optimal leaf temperature in terrestrial plants. *Nat Commun.*, 14, 2820. DOI: 10.1038/s41467-023-38496-4

Schmiege S.C., Griffin K.L., Boelman N.T., Vierling L.A., Bruner S.G., Min E., Maguire A.J., Jensen J., Eitel J.U.H. (2023). Vertical gradients in photosynthetic physiology diverge at the latitudinal range extremes of white spruce. *Plant Cell Environ.*, 46, 45–63. DOI: 10.1111/pce.14448

Sellin A., Alber M., Jasińska A.K., Rosenvald K. (2022). Adjustment of leaf anatomical and hydraulic traits across vertical canopy profiles of young broadleaved forest stands. *Trees*, 36, 67–80. DOI: 10.1007/s00468-021-02181-0

Sellin A., Taneda H., Alber M. (2019). Leaf structural and hydraulic adjustment with respect to air humidity and canopy position in silver birch (*Betula pendula*). *J Plant Res.*, 132, 369–381. DOI: 10.1007/s10265-019-01106-w

Sharkey T.D. (1985). Photosynthesis in intact leaves of C<sub>3</sub> plants: physics, physiology and rate limitations. *The Botanical Review*, 51, 53–105. DOI: 10.1007/BF02861058

Sharkey T.D. (2016). What gas exchange data can tell us about photosynthesis. *Plant Cell Environ*, 39, 1161–1163. DOI: 10.1111/pce.12641

Sharkey T.D. (2024). The end game(s) of photosynthetic carbon metabolism. *Plant Physiol*, 195(1), 67–78. DOI: 10.1093/plphys/kiad601

Sharkey T.D., Bernacchi C.J., Farquhar G.D., Singsaas E.L. (2007). Fitting photosynthetic carbon dioxide response curves for C<sub>3</sub> leaves. *Plant Cell Environ*, 30, 1035–1040. DOI: 10.1111/j.1365-3040.2007.01710.x.

Shiklomanov A.N., Cowdery E.M., Bahn M., Byun C., Jansen S., Kramer K., Minden V., Niinemets U., Onoda Y., Soudzilovskaia N.A., Dietze M.S. (2020). Does the leaf economic spectrum hold within plant functional types? A Bayesian multivariate trait meta-analysis. *Ecological application*, 30(3), 1–15. DOI: 10.1002/eap.2064

Stribet A., Guo Y., Lazár D., Govindjee G. (2024). From leaf to multiscale models of photosynthesis: applications and challenges for crop improvement. *Photosynth Res*, 161, 21–49. DOI: 10.1007/s11120-024-01083-9

Sukhova E.M., Vodeneev V.A., Sukhov V.S. (2021). Mathematical modeling of photosynthesis and analysis of plant productivity. *Biochem Moscow Suppl Ser A*, 15, 52–72. DOI: 10.1134/S1990747821010062

Suvorova G.G., Popova E.V. (2015). Photosynthetic productivity of coniferous stands of the Irkutsk region. Novosibirsk, Geo, 95 p. (In Russian)

Togashi H.F., Prentice I.C., Atkin O.K., Macfarlane C., Prober S.M., Bloomfield K.J., Evans B.J. (2018). Thermal acclimation of leaf photosynthetic traits in an evergreen woodland, consistent with the coordination hypothesis. *Biogeosciences*, 15(11), 3461–3474. DOI: 10.5194/bg-15-3461-2018

Tselniker Yu.L. (1982). A simplified method for determination of needle surface in pine and spruce trees. *Russ J Forest Sci*, 4, 85–88. (In Russian)

Tselniker Yu.L., Malkina I.S., Kovalev A.G., Chmora S.N., Mamaev V.V., Molchanov A.G. (1993). The growth and CO<sub>2</sub>-exchange in forest trees. Nauka, Moskva, 256 p. (In Russian)

Vasfilov S.P. (2016). The effect of photosynthesis parameters on leaf lifespan. *Biol Bull Rev*, 6(1), 96–112. DOI: 10.1134/S2079086416010084

Veromann-Jürgenson L.-L., Tosens T., Laanisto L., Niinemets U. (2017). Extremely thick cell walls and low mesophyll conductance: welcome to the world of ancient living! *J Experimental Botany*, 68(7), 1639–1653. DOI: 10.1093/jxb/erx045

Vogel C.S., Curtis P.S. (1995). Leaf gas exchange and nitrogen dynamics of N<sub>2</sub>-fixing, field-grown *Alnus glutinosa* under elevated atmospheric CO<sub>2</sub>. *Glob Change Biol*, 1, 55–61. DOI: 10.1111/j.1365-2486.1995.tb00006.x

Von Caemmerer S. (2000). Biochemical models of leaf photosynthesis. CSIRO publishing, 165 p. DOI: 10.1071/9780643103405

Wullschleger S.D. (1993). Biochemical limitations to carbon assimilation in C<sub>3</sub>-plants – a retrospective analysis of the A/Ci curves from 109 species. *J Experimental Botany*, 44(5), 907–920.